MATERIALS CHEMISTRY FRONTIERS

Digestive Ripening in the Formation of Monodisperse Silver Nanospheres

Journal:	*Materials Chemistry Frontiers*
Manuscript ID	QM-RES-02-2018-000077.R1
Article Type:	Research Article
Date Submitted by the Author:	03-Apr-2018

Complete List of Authors:	Zhang, Shumeng; Xi'an Jiaotong University, Frontier Institute of Science and Technology Zhang, Lei; Xi'an Jiaotong University, Liu, Kai; Xi'an Jiaotong University, Frontier Institute of Science and Technology Liu, Moxuan; Xi'an Jiaotong University, Frontier Institute of Science and Technology Yin, Yadong; University of California Riverside, Department of Chemistry Gao, Chuanbo; Xi'an Jiaotong University, Frontier Institute of Science and Technology

Materials Chemistry Frontiers

REARCH ARTICLE

Digestive Ripening in the Formation of Monodisperse Silver Nanospheres

Shumeng Zhang,[a]† Lei Zhang,[a]† Kai Liu,[a] Moxuan Liu,[a] Yadong Yin[b] and Chuanbo Gao*[a]

Received 00th January 20xx,
Accepted 00th January 20xx

DOI: 10.1039/x0xx00000x

www.rsc.org/

Digestive ripening is a unique process in colloidal synthesis that can enable direct conversion of polydisperse nanoparticles into monodisperse ones. However, such a strategy usually relies on strongly coordinating ligands such as alkylthiols to initiate etching and stabilize the surfaces and thus affords nanoparticles with hydrophobic and passivated surfaces, which greatly limits their applications. In this work, we report that digestive ripening can be achieved by decoupling the etching and surface stabilization functions using two independent chemical agents, allowing the use of considerably weak capping ligands which are hydrophilic and can be replaced later according to the need of the specific applications. As a proof-of-concept, we, for the first time, demonstrate a novel digestive ripening system to synthesize hydrophilic monodisperse Ag nanospheres capped by conveniently removable ligands. With chloride for oxidative etching and diethylamine for effective surface capping, monodisperse Ag nanospheres have been conveniently obtained by starting with a precursor of either a Ag^+ solution or a AgCl suspension. These monodisperse Ag nanospheres with a clean surface exhibit excellent activity in surface-enhanced Raman scattering (SERS). We believe the new strategy may significantly broaden the general applicability of the digestive ripening for the controlled synthesis of colloidal nanoparticles for a broad range of applications.

Introduction

Digestive ripening is a unique post-synthetic process that allows the conversion of polydisperse nanoparticles into monodisperse ones.[1] Different from an Ostwald ripening process that induces the growth of large nanoparticles at the expense of smaller ones, the digestive ripening process involves the etching or dissolution of large nanoparticles and the growth of smaller ones in the presence of a strongly coordinating ligand in excess, leading to significant narrowing of the particle size distribution.[2-4] One unique feature of this process is that albeit different initial sizes of the nanoparticles, a thermodynamically equilibrium size[3-5] of the nanoparticles is usually obtained that depends on the specific ligand and the reaction temperature,[2-10] demonstrating high yield and reproducibility. Therefore, digestive ripening represents an effective and reliable pathway to synthesize nanoparticles with high monodispersity, which paves a way to the research on the size-dependent properties of nanoparticles and to the pursuit of their consistent performance in practical applications.[1, 4-19]

However, state-of-the-art digestive ripening syntheses are most successful in the synthesis of hydrophobic Au nanoparticles[1, 4-14] by relying on the strong interaction between Au nanoparticles and strongly coordinating ligands such as long-chain alkylthiols, amines and phosphines.[7] Therefore, this process is usually carried out in a nonpolar solvent such as benzene, toluene, chloroform and dichlorobenzene.[3] The roles of the strongly coordinating ligand in the digestive ripening process are two-fold: it serves as an etchant for the Au nanoparticles to enable their effective dissolution, and it is also a capping agent to reduce the surface energy of the Au nanoparticles.[5, 20] However, it leads to significant passivation of the nanoparticle surface and insolubility of the nanoparticles in many polar solvents, which greatly limits the use of these nanoparticles in many applications such as bio-sensing, labelling, imaging, and catalysis. In addition, the digestive ripening processes are usually conducted at the boiling temperature of the solvent, which is energy-consuming.[3, 9, 10] For the synthesis of metal nanoparticles targeting primarily at biomedical and catalytic applications, an ideal digestive ripening process should be conducted preferably in a polar solvent under a mild condition, using a hydrophilic ligand that can be conveniently replaced.

To address this issue, in this work, we report that the digestive ripening can be achieved by decoupling the etching and surface stabilization by two independent hydrophilic chemical agents, which avoids the use of hydrophobic strongly-coordinating ligands and enables us to synthesize monodisperse metal nanoparticles with a hydrophilic, exchangeable surface. As a proof-of-concept, for the first time, we demonstrate that hydrophilic monodisperse Ag nanospheres (diameter: 9–15 nm) could be synthesized in a polar solvent of *N*, *N*-dimethylformamide (DMF)[21] by employing chloride (Cl^-) for the

[a] Frontier Institute of Science and Technology, and State Key Laboratory of Multiphase Flow in Power Engineering, Xi'an Jiaotong University, Xi'an, Shaanxi 710054, China. Email: gaochuanbo@mail.xjtu.edu.cn
[b] Department of Chemistry, University of California, Riverside, California 92521, United States.
† These authors contributed equally to this work
Electronic Supplementary Information (ESI) available: UV-vis and TEM results of the control experiments to support the mechanism of the digestive ripening synthesis; Additional Raman spectra. See DOI: 10.1039/x0xx00000x

oxidative etching of the Ag nanoparticles[22, 23] and diethylamine (DEA) for the surface stabilization,[24, 25] starting from either a Ag^+ solution or a AgCl suspension. Thus, this novel system allows the use of considerably weak capping ligands that could be replaced later according to the need of specific applications. This study provides a robust method to synthesize monodisperse water-soluble Ag nanospheres in high yield and quality, which may find broad applications in surface-enhanced Raman scattering (SERS),[26-28] bio-sensing,[24] imaging,[29] and photocatalysis.[30, 31] We believe the findings gained in this work may also help to advance the understanding of the digestive ripening process and significantly broaden its general applicability for the controlled synthesis of colloidal nanoparticles.

Results and Discussion

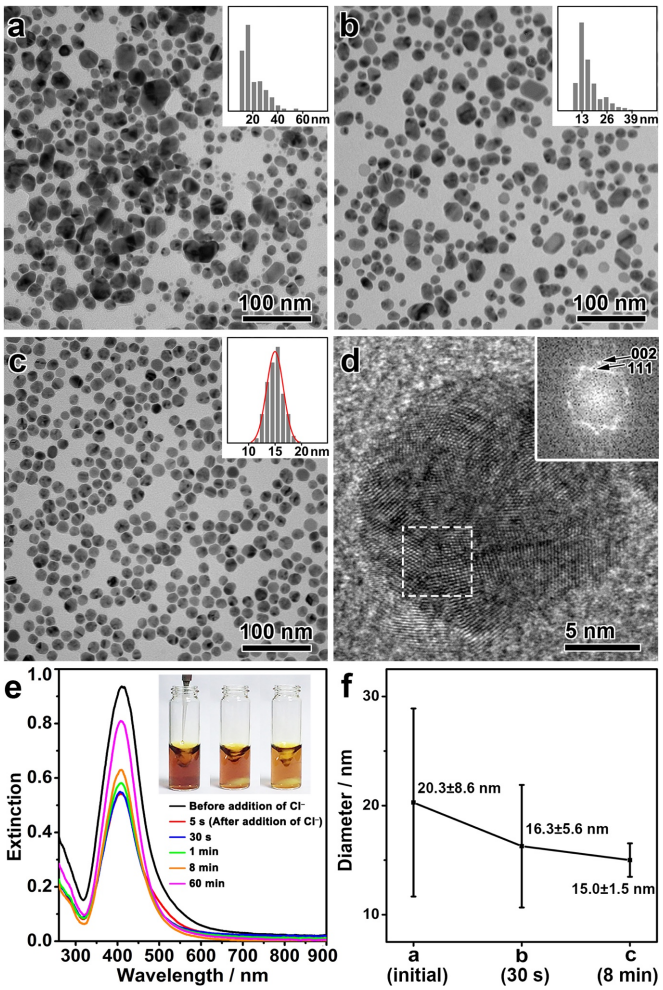

Figure 1. A digestive ripening route to monodisperse Ag nanospheres. (a–c) TEM images of the Ag nanoparticles obtained before the addition of Cl^-, at 30 s and 8 min after the addition of Cl^-, respectively. Inset: Size distributions of the Ag nanoparticles. (d) HRTEM image of an individual Ag nanosphere. Inset: Fourier diffractogram, corresponding to the dashed square area. (e) UV-vis extinction spectra of the Ag nanoparticles recorded during the synthesis. Inset: photographs of the Ag sols obtained before the digestive ripening, at 5 s and 30 s after the addition of Cl^-, respectively, from left to right. (f) Change of the size (diameter) and size distribution of the Ag nanoparticles during the digestive ripening, corresponding to (a–c). The error bars indicate the standard deviation for each diameter.

In a typical synthesis, polydisperse Ag nanospheres were first prepared by a chemical reduction method. Upon mixing polyvinylpyrrolidone (PVP), DEA, and $AgNO_3$ in DMF in sequence under vigorous stirring, a yellow sol of the Ag nanospheres was obtained. Here, DEA could be partially oxidized to produce diethylhydroxylamine (DEHA) under the aerobic condition, which served as the reducing agent to afford polydisperse Ag nanoparticles (Figure S1, ESI†).[32] The presence of PVP, a commonly used surfactant, ensured the colloidal property of the Ag nanoparticles (Figure S2, ESI†). Then, sodium chloride (NaCl) was introduced into the Ag sol, which, together with DEA, initiated the digestive ripening process. The reaction system was then transferred to a water bath at 50 °C and stirred for 8 min, producing monodisperse Ag nanospheres as a final product.

Figure 1(a–c) shows the transmission electron microscopy (TEM) images of the intermediates formed at different stages of the synthesis. After the chemical reduction, Ag nanoparticles were obtained with a broad size distribution, showing the presence of both small (< 20 nm) and large Ag nanoparticles (20–60 nm) (Figure 1a). After the addition of NaCl, the population of the large Ag nanoparticles was significantly reduced, leading to a decrease in the mean size of the nanoparticles and a significant narrowing of the size distribution even after a very short reaction time (Figure 1b, for the intermediate after 30 s of the reaction). A prolonged reaction time allowed further narrowing of the size distribution, and monodisperse Ag nanospheres were eventually obtained in 8 min (Figure 1c, a low-magnification TEM image see Figure S3, ESI†). It is inferred that during the whole process, large nanoparticles were selectively etched, which led to a size focusing to a small value, typical of a digestive ripening phenomenon. Figure 1f summarizes the size distributions of the Ag nanoparticles during the digestive ripening process. The size distribution started from a high standard deviation of 8.6 nm (42.5% of the mean size, 20.3 nm), which underwent a continuous decrease during the digestive ripening. The standard deviation was reduced to 1.5 nm (10% of the mean size, 15.0 nm) after 8 min, confirming the excellent monodispersity of the resulting Ag nanospheres. The high-resolution TEM (HRTEM) image and the corresponding Fourier diffractogram suggest that the resulting Ag nanospheres are polycrystalline nanocrystals (Figure 1d).

The digestive ripening process of the Ag nanospheres can be monitored by UV-vis spectroscopy (Figure 1e). Before the ripening, the polydisperse Ag nanoparticles exhibited an extinction band at ~ 412 nm due to the strong localized surface plasmon resonance (LSPR). After the addition of NaCl, significantly decreased intensity of the extinction band can be observed accompanying the oxidative etching process of the Ag nanoparticles. After ~ 1 min, the intensity of the extinction band began to increase slowly, which suggests a regrowth of the Ag nanoparticles resulting from a further reduction of the Ag salt released by the etching process. It is worth noting that the regrowth continued for more than 60 min, indicating that a high concentration of Ag salt was present in the reaction as a result of the etching of the large Ag nanoparticles.

Further study was conducted to understand the mechanism of this unique digestive ripening process. In this system, the chloride is believed to account for the oxidative etching of the Ag nanoparticles under the aerobic condition.[22, 23] It can be confirmed by degassing O_2 from a typical digestive ripening system, which leads to suppressed etching of the Ag nanoparticles (Figure S4, ESI†). Our experiments also show that DEA plays a central role in enabling the etching selectivity of the Cl^-/O_2 toward the large Ag nanoparticles. If DEA is neutralized by acetic acid before a typical digestive ripening process, subsequent addition of the chloride leads to etching of Ag nanoparticles of small sizes and retention of large ones, producing Ag nanoparticles with an increased mean size (38.4 nm) and a broad size distribution (standard deviation, 9.9 nm, ~ 25% of the mean size), in clear contrast to the typical process with DEA (Figure 2a, b). As found in our previous reports,[24, 25, 32] DEA can strongly adsorb on the Ag nanoparticles to reduce the surface energy (Figure S5, ESI†). We believe that the reduction of the surface energy due to the DEA adsorption depends on the size of the Ag nanoparticles, which increases with a decreasing size of the nanoparticles. However, the decrease in the particle size also leads to significantly increased surface area and consequently surface energy. Therefore, an equilibrium size of the Ag nanoparticles could be achieved at a minimum surface energy, which accounts for the selective etching of Ag nanoparticles of large sizes and the formation of monodisperse Ag nanospheres.[3]

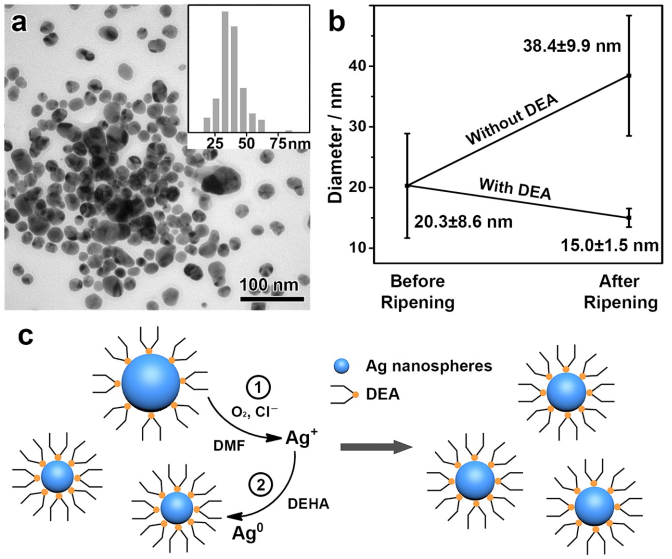

Figure 2. The role of DEA in the digestive ripening process. (a) TEM image of the Ag nanoparticles obtained from a control synthesis with DEA neutralized before the ripening process. Inset: size distribution of the Ag nanoparticles. (b) Change of the size of the Ag nanoparticles with or without DEA. The error bars indicate the standard deviation of the particle size. (c) A cartoon illustrating the formation mechanism of monodisperse Ag nanospheres by the digestive ripening and subsequent regrowth.

In addition, DMF as a solvent is also an important driving factor for the digestive ripening of the Ag nanoparticles. As indicated by a previous study,[33] DMF is capable of coordinating to metal ions such as Ag(I), which makes it possible to accommodate a high concentration of AgCl during the oxidative etching so that the digestive ripening can proceed much more easily in DMF than in many other solvents. For comparison, no significant digestive ripening phenomenon could be observed when the synthesis is conducted in water (Figure S6, ESI†).

Therefore, a reasonable mechanism can be proposed to rationalize this unique digestive ripening system (Figure 2c). First, polydisperse Ag nanospheres were obtained and stabilized by DEA, with Ag nanoparticles of large sizes binding DEA more weakly than those of small ones. Upon the introduction of Cl^-/O_2, oxidative etching occurs selectively to Ag nanoparticles of large sizes. The resulting AgCl was well accommodated by DMF, which allows the continuous oxidative etching, leading to monodisperse Ag nanospheres of an equilibrium size depending on the binding energy of the Ag nanoparticles with DEA. In addition, the AgCl accommodated by DMF is capable of further reduction and regrowth on the existing Ag nanospheres, making it possible to synthesize monodisperse Ag nanospheres with controllable sizes.

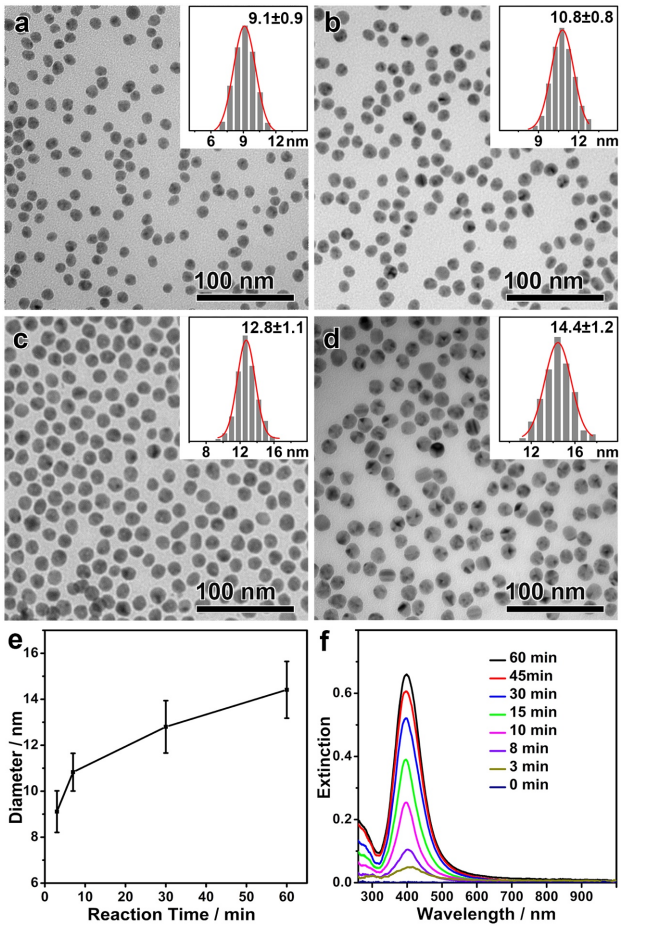

Figure 3. Control over the size of the monodisperse Ag nanospheres through the digestive ripening. (a–d) TEM images of the Ag nanospheres obtained after stirring at 50 °C for 3 min, 7 min, 30 min, and 60 min, respectively. Inset: size distributions of the Ag nanospheres. The means sizes are expressed in terms of "mean ± standard deviation". (e) Change of the mean size of the monodisperse Ag nanospheres with the reaction time. The error bars indicate the standard deviations for each point. (f) UV-vis extinction spectra of the Ag nanospheres as a function of the reaction time.

As discussed above, the monodisperse Ag nanospheres were obtained with an equilibrium size, which suggests that the formation of the Ag nanospheres is independent of the reaction pathway. It is predicted that the same monodisperse Ag nanospheres could be obtained in a much more convenient way by convoluting the formation of Ag nanoparticles and the digestive ripening process in one step. In a typical modified synthesis, all chemicals including PVP, DEA, $AgNO_3$ and NaCl were added to the solvent DMF, and the solution was first stirred at room temperature for 5 min and then at 50 °C for different lengths of time. As expected, monodisperse Ag nanospheres with an equilibrium size of ~ 9 nm were obtained after a very short reaction time (Figure 3a). A high concentration of AgCl in DMF enabled continuous growth of the monodisperse Ag nanospheres in the following step, giving rise to monodisperse Ag nanospheres with continuously increasing sizes (Figure 3b–d). By this means, the mean size of the monodisperse Ag nanospheres could be conveniently tuned in a range of 9–15 nm, all showing narrow size distributions (standard deviation, < 10%) (Figure 3e). The intensity of the LSPR band increased continuously with time, suggesting an increasing concentration and/or size of the Ag nanospheres (Figure 3f). No drops in the intensity of the LSPR band can be observed during the whole synthesis (as observed in Figure 1e), which confirms that the chemical reduction and the digestive ripening occurred without in a temporal sequence.

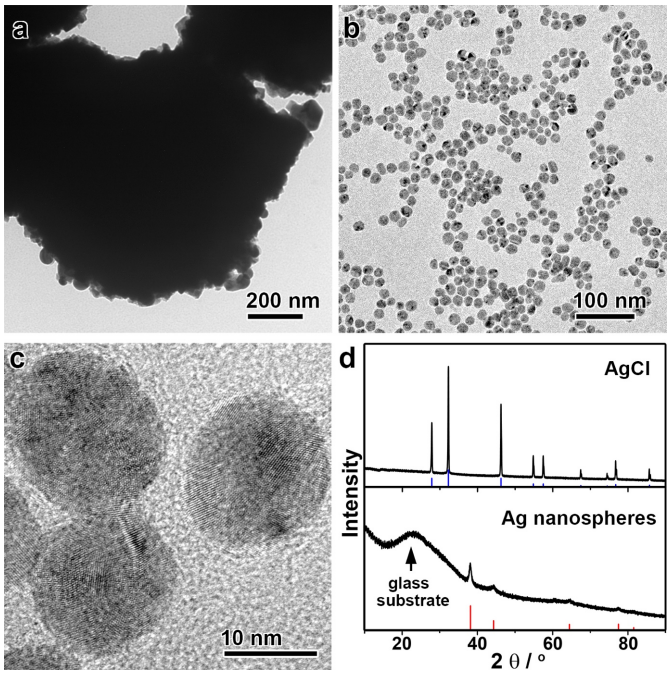

Figure 4. Synthesis of monodisperse Ag nanospheres starting from a AgCl precursor. (a–b) TEM images of the AgCl precipitate and the resulting monodisperse Ag nanospheres. (c) HRTEM image of the monodisperse Ag nanospheres. (d) XRD patterns of the AgCl precipitate and the monodisperse Ag nanospheres. Standard peak positions of Ag (red sticks, JCPDF #04-0783) and AgCl (blue sticks, JCPDF #31-1238) are listed for reference.

Interestingly, this unique digestive ripening mechanism allows direct conversion of a AgCl suspension into monodisperse Ag nanospheres (Figure 4). It is not of surprise that one can produce Ag nanoparticles by reducing AgCl solids, albeit with broad size distributions. However, as Cl^- ions are released after the chemical reduction, they together with DEA can initiate the effective digestive ripening process to afford monodisperse Ag nanospheres. In this case, the AgCl solid serves as both the Ag source and the Cl source. Because the digestive ripening is a thermodynamic process, the use of a AgCl solid in place of $AgNO_3$ as the precursor does not exert a significant influence on the equilibrium size of the monodisperse Ag nanospheres. Figure 4a–c shows the TEM images of the AgCl precipitate and the monodisperse Ag nanospheres obtained from this synthesis. Although the AgCl precipitate is micron-sized as a precursor (Figure 4a), the resulting Ag nanospheres are highly uniform with a mean size of ~15 nm (Figure 4b–c). The complete transformation of the AgCl solid into monodisperse Ag nanospheres can be further confirmed by X-ray diffraction (XRD) (Figure 4d). The direct conversion of AgCl solids into monodisperse Ag nanospheres not only provides a direct evidence to support the digestive ripening mechanism, but also offers a robust method for the convenient preparation of Ag nanospheres in a high quality and yield in a very economical way.

This digestive ripening process is also applicable to the synthesis of monodisperse Ag-Au alloy nanospheres (Figure S7, ESI†). At a high ratio of Ag/Au (larger than 5), the Ag-Au alloy nanoparticles become less stable and susceptible to chemical etching by Cl^-/O_2, which is pre-requisite for a digestive ripening mechanism. As a result, the LSPR band of the monodisperse nanospheres can be conveniently tuned by the Ag/Au ratio in the alloy nanospheres.

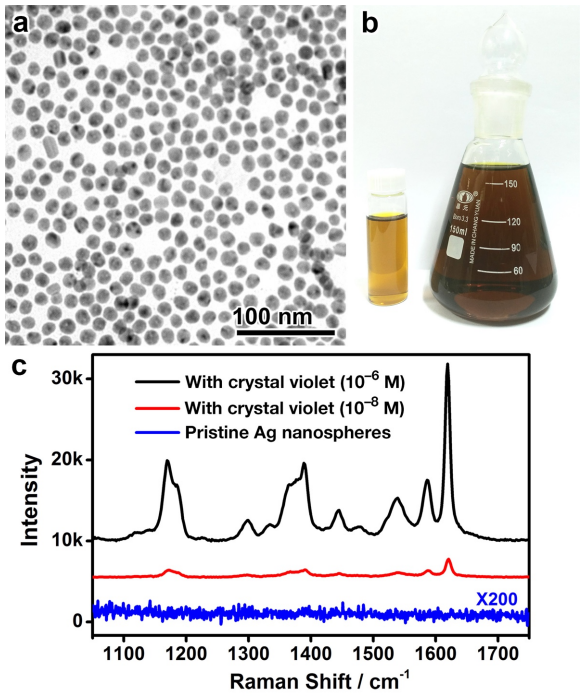

Figure 5. (a–b) Large-scale synthesis of monodisperse Ag nanospheres (target size: 13 nm) by digestive ripening, which yields ~ 54 mg of the final product from one pot. (a) TEM image of the Ag nanospheres. (b) A photograph of the Ag colloid. (c) SERS spectra of crystal violet with a concentration of 10^{-6} M and 10^{-8} M recorded from the substrate of the Ag nanospheres. Raman spectrum of the Ag substrate without crystal violet was also listed, confirming the clean surface of the Ag nanospheres.

As one advantage of this digestive ripening synthesis, we further show that it can be readily scaled up to produce a large quantity of monodisperse Ag nanospheres under mild reaction conditions. In a typical demonstration, 54 mg of monodisperse Ag nanospheres with a target size of ~13 nm (corresponding to Figure 3c) have been synthesized by scaling up a typical synthesis in the Materials and Methods section for 20 times (Figure 5a–b). TEM imaging suggests that the Ag nanospheres obtained from the large-scale synthesis were of high monodispersity, with the mean size being almost identical to the target size, confirming excellent reproducibility of the method in a large scale synthesis without losing the overall quality.

More importantly, as no strongly coordinating ligands are involved in this digestive ripening process, it is capable of producing monodisperse Ag nanospheres with a hydrophilic surface and conveniently removable capping ligands (specifically, DEA and PVP). To confirm this significant advantage, the monodisperse Ag nanospheres (9 nm) were dried on a silicon substrate, washed with water, and subjected to surface-enhanced Raman scattering (SERS) analysis. No obvious SERS signals could be detected from the surface ligands, suggesting that the ligands (DEA and PVP) have been effectively removed from the Ag surface by washing with water (Figure 5c and Figure S8, ESI†). The surfactant-free surface of the resulting Ag nanospheres enables excellent SERS activity in detecting molecules of interest, crystal violet for example, in ultralow concentrations (Figure 5c). It is worth noting that the excellent SERS activity of the Ag nanospheres may be partially attributed to the presence of chloride on the Ag surface (Figure S9, ESI†), which is commonly observed in literature.[34, 35] We believe these monodisperse Ag nanospheres could find use in a much broader range of applications, such as biosensing, imaging, and fabrication of optical and electrical nanodevices.

Materials and methods

Material.

N, *N*-Dimethyl formamide (DMF), silver nitrate ($AgNO_3$, 99%), polyvinylpyrrolidone (PVP, Mw 29000), diethylamine (DEA), acetic acid, and sodium chloride (NaCl) were purchased from Sigma-Aldrich and used as received.

Synthesis of monodisperse Ag nanospheres by digestive ripening.

In a typical synthesis, 400 µL of PVP (Mw 29000, 5 wt% in DMF), 80 µL of DEA and 250 µL of $AgNO_3$ (0.1 M) were added to 8.4 mL of DMF in sequence under vigorous stirring at room temperature (24 °C). The reaction solution was stirred at room temperature for 5 min and 50 °C for 30 min, giving rise to polydisperse Ag nanospheres. Then, 10 µL of NaCl (1 M) was added to the reaction system to initiate the digestive ripening process. After 30 min, monodisperse Ag nanospheres were formed, which were then collected by centrifugation and washed with water.

A modified digestive ripening route to monodisperse Ag nanospheres with tunable sizes.

In a typical synthesis, 400 µL of PVP (Mw 29000, 5 wt% in DMF), 80 µL of DEA, 250 µL of $AgNO_3$ (0.1 M) and 10 µL of NaCl (1 M) were added to 8.4 mL of DMF in sequence under vigorous stirring at room temperature. The reaction solution was stirred at room temperature for 5 min and 50 °C for a different length of time, giving rise to monodisperse Ag nanospheres. The Ag nanospheres were finally collected by centrifugation and washed with water. The size of the Ag nanospheres can be tuned by adjusting the reaction time at 50 °C, and Ag nanospheres of 9, 11, 13 and 15 nm were obtained after reaction for 3, 7, 30, and 60 min, respectively.

Synthesis of monodisperse Ag nanospheres starting from AgCl.

First, a AgCl suspension was prepared by mixing 250 µL of $AgNO_3$ (0.1 M) with 20 µL of NaCl (2.5 M). In a typical synthesis, a solution was prepared by incorporating 400 µL of PVP (Mw 29000, 5 wt% in DMF), 80 µL of DEA and 8.4 mL of DMF in a glass vial, which was then merged with the AgCl precipitate and stirred at 50 °C for 1 h. The resulting monodispersed Ag nanospheres were centrifuged and washed with H_2O.

Surface-enhanced Raman spectroscopy (SERS).

The substrates for SERS were prepared by dropping and drying a known quantity of Ag nanospheres on a clean silicon wafer (8 mm × 8 mm). In a typical SERS experiment, 25 µL of crystal violate (CV) (10^{-6} M or 10^{-8} M) was dropped and dried on the substrate. Raman spectra were recorded by using a LabRAM HR800 confocal Raman spectrophotometer equipped with a 532 nm He–Ne laser line at room temperature. For all measurements, laser spots were 0.72 µm under a 100× objective, power of the laser spot was 1 mW, and the signal acquisition time was 1 s.

Characterizations.

Transmission electron microscopy (TEM) was performed on a Hitachi HT-7700 microscope operated at an accelerating voltage of 100 kV. High-resolution TEM (HRTEM) analysis was performed on a Philips Tecnai F20 FEG-TEM microscope operated at an accelerating voltage of 200 kV. X-ray diffraction (XRD) patterns were recorded on a Rigaku SmartLab X-ray diffractometer equipped with Cu Kα radiation and D/teX Ultra detector, scanning from 10° to 90° (2ϑ) at the rate of 10° min^{-1}. UV-vis spectroscopy was performed on an Ocean Optics HR2000+ES UV-vis-NIR spectrophotometer with a DH-2000-Bal light source.

Conclusions

In summary, we take the synthesis of Ag nanoparticles as a proof-of-concept, and demonstrate that digestive ripening can be successfully realized by decoupling the etching and surface stabilization functions using two independent chemical agents, which avoids the surface passivation of nanoparticles by a hydrophobic strongly coordinating ligand as used in a

conventional synthesis, and affords hydrophilic monodisperse nanoparticles with considerably weak capping ligands that are conveniently exchangeable for different applications. The clean surface of the resulting Ag nanospheres enables excellent SERS activity in detecting molecules of interest in ultralow concentrations. We believe the new strategy not only provides a unique and robust method for the synthesis of monodisperse Ag nanospheres,[36-40] but also helps to advance the understanding of the digestive ripening process that remains elusive to date, which may significantly broaden the general applicability of this important strategy for the controlled synthesis of colloidal nanoparticles.

Conflicts of interest

There are no conflicts to declare.

Acknowledgements

C.G. acknowledges the support from the National Natural Science Foundation of China (21671156, 21301138), the Tang Scholar Program from Cyrus Tang Foundation, and the start-up fund from Xi'an Jiaotong University. Y.Y. acknowledges the support from the U.S. National Science Foundation (CHE-1308587).

Notes and references

1. X. M. Lin, C. M. Sorensen and K. J. Klabunde, *J. Nanopart. Res.*, 2000, **2**, 157-164.
2. J. R. Shimpi, D. S. Sidhaye and B. L. V. Prasad, *Langmuir*, 2017, **33**, 9491-9507.
3. J. A. Manzanares, P. Peljo and H. H. Girault, *J. Phys. Chem. C*, 2017, **121**, 13405-13411.
4. S. P. Bhaskar, M. Vijayan and B. R. Jagirdar, *J. Phys. Chem. C*, 2014, **118**, 18214-18225.
5. D. Jose, J. E. Matthiesen, C. Parsons, C. M. Sorensen and K. J. Klabunde, *J. Phys. Chem. Lett.*, 2012, **3**, 885-890.
6. B. L. V. Prasad, S. I. Stoeva, C. M. Sorensen and K. J. Klabunde, *Langmuir*, 2002, **18**, 7515-7520.
7. B. L. V. Prasad, S. I. Stoeva, C. M. Sorensen and K. J. Klabunde, *Chem. Mater.*, 2003, **15**, 935-942.
8. H. Hiramatsu and F. E. Osterloh, *Chem. Mater.*, 2004, **16**, 2509-2511.
9. P. Sahu and B. L. Prasad, *Nanoscale*, 2013, **5**, 1768-1771.
10. P. Sahu, J. Shimpi, H. J. Lee, T. R. Lee and B. L. Prasad, *Langmuir*, 2017, **33**, 1943-1950.
11. N. Zheng, J. Fan and G. D. Stucky, *J. Am. Chem. Soc.*, 2006, **128**, 6550-6551.
12. S. I. Stoeva, A. B. Smetana, C. M. Sorensen and K. J. Klabunde, *J. Colloid Interface Sci.*, 2007, **309**, 94-98.
13. M.-L. Lin, F. Yang, J. S. Peng and S. Lee, *J. Appl. Phys.*, 2014, **115**, 054312.
14. Q. Zhang, J. Xie, J. Yang and J. Y. Lee, *ACS Nano*, 2009, **3**, 139-148.
15. A. B. Smetana, K. J. Klabunde and C. M. Sorensen, *J. Colloid Interface Sci.*, 2005, **284**, 521-526.
16. A. B. Smetana, K. J. Klabunde, C. M. Sorensen, A. A. Ponce and B. Mwale, *J. Phys. Chem. B*, 2006, **110**, 2155-2158.
17. D. Heroux, A. Ponce, S. Cingarapu and K. J. Klabunde, *Adv. Funct. Mater.*, 2007, **17**, 3562-3568.
18. S. B. Kalidindi and B. R. Jagirdar, *Inorg. Chem.*, 2009, **48**, 4524-4529.
19. R. Shankar, B. B. Wu and T. P. Bigioni, *J. Phys. Chem. C*, 2010, **114**, 15916-15923.
20. T. G. Schaaff and R. L. Whetten, *J. Phys. Chem. B*, 1999, **103**, 9394-9396.
21. I. Pastoriza-Santos and L. M. Liz-Marzán, *Adv. Funct. Mater.*, 2009, **19**, 679-688.
22. B. Wiley, T. Herricks, Y. Sun and Y. Xia, *Nano Lett.*, 2004, **4**, 1733-1739.
23. J. Seth and B. L. V. Prasad, *Nano Res.*, 2016, **9**, 2007-2017.
24. C. Gao, Z. Lu, Y. Liu, Q. Zhang, M. Chi, Q. Cheng and Y. Yin, *Angew. Chem. Int. Ed.*, 2012, **51**, 5629-5633.
25. Q. Fan, K. Liu, Z. Liu, H. Liu, L. Zhang, P. Zhong and C. Gao, *Part. Part. Syst. Charact.*, 2017, **34**, 1700075.
26. S. Nie and S. R. Emory, *Science*, 1997, **275**, 1102-1106.
27. S. Schlücker, *Angew. Chem. Int. Ed.*, 2014, **53**, 4756-4795.
28. M. Rycenga, C. M. Cobley, J. Zeng, W. Li, C. H. Moran, Q. Zhang, D. Qin and Y. Xia, *Chem. Rev.*, 2011, **111**, 3669-3712.
29. K.-S. Lee and M. A. El-Sayed, *J. Phys. Chem. B*, 2006, **110**, 19220-19225.
30. K. Awazu, M. Fujimaki, C. Rockstuhl, J. Tominaga, H. Murakami, Y. Ohki, N. Yoshida and T. Watanabe, *J. Am. Chem. Soc.*, 2008, **130**, 1676-1680.
31. P. Christopher, H. Xin and S. Linic, *Nat. Chem.*, 2011, **3**, 467-472.
32. L. Zhang, X. Sha, Q. Fan, L. Han, Y. Yin and C. Gao, *Nanoscale*, 2017, **9**, 17037-17043.
33. J. N. Butler, *J. Phys. Chem.*, 1968, **72**, 3288-3292.
34. A. M. Michaels, M. Nirmal and L. E. Brus, *J. Am. Chem. Soc.*, 1999, **121**, 9932-9939.
35. E. J. Liang, C. Engert and W. Kiefer, *Vib. Spectrosc.*, 1995, **8**, 435-444.
36. P. C. Lee and D. Meisel, *J. Phys. Chem.*, 1982, **86**, 3391-3395.
37. Y. X. Hu, J. P. Ge, D. Lim, T. R. Zhang and Y. D. Yin, *J. Solid State Chem.*, 2008, **181**, 1524-1529.
38. X. Liu, Y. Yin and C. Gao, *Langmuir*, 2013, **29**, 10559-10565.
39. H. Li, H. Xia, D. Wang and X. Tao, *Langmuir*, 2013, **29**, 5074-5079.
40. N. G. Bastús, F. Merkoçi, J. Piella and V. Puntes, *Chem. Mater.*, 2014, **26**, 2836-2846.